

Highly Efficient Asymmetric Synthesis of Sitagliptin

Karl B. Hansen,^{*,†} Yi Hsiao,^{*,†} Feng Xu,^{*,†} Nelo Rivera,[†] Andrew Clausen,[†]
 Michele Kubryk,[†] Shane Krska,[†] Thorsten Rosner,[†] Bryon Simmons,[†]
 Jaime Balsells,[†] Nori Ikemoto,[†] Yongkui Sun,[†] Felix Spindler,[‡] Christophe Malan,[‡]
 Edward J. J. Grabowski,[†] and Joseph D. Armstrong III.[†]

*Department of Process Research, Merck Research Laboratory, Rahway, New Jersey 07065, and
 Solvias AG, P.O. Box 4002, Basel, Switzerland*

Received April 3, 2009; E-mail: feng_xu@merck.com; joe_armstrong@merck.com

Abstract: A highly efficient synthesis of sitagliptin, a potent and selective DPP-4 inhibitor for the treatment of type 2 diabetes mellitus (T2DM), has been developed. The key dehydrositagliptin intermediate **9** is prepared in three steps in one pot and directly isolated in 82% yield and >99.6 wt % purity. Highly enantioselective hydrogenation of dehydrositagliptin **9**, with as low as 0.15 mol % of Rh(I)/Bu JOSIPHOS, affords sitagliptin, which is finally isolated as its phosphate salt with nearly perfect optical and chemical purity. This environmentally friendly, 'green' synthesis significantly reduces the total waste generated per kilogram of sitagliptin produced in comparison with the first-generation route and completely eliminates aqueous waste streams. The efficiency of this cost-effective process, which has been implemented on manufacturing scale, results in up to 65% overall isolated yield.

Introduction

Type 2 diabetes mellitus (T2DM) is a global epidemic. The number of reported cases has doubled over the past 15 years.¹ Recently, dipeptidyl peptidase IV (DPP-4) inhibitors have emerged as a new class of antihyperglycemic agents for the treatment of T2DM² and offer several advantages over other existing antidiabetic agents such as lack of body weight gain and decreased incidence of hypoglycemic episodes. Sitagliptin (**1**),³ a selective, potent DPP-4 inhibitor, is the active ingredient in JANUVIA and JANUMET (a fixed dose combination with the antidiabetic agent metformin), which both recently received approval for the treatment of type 2 diabetes by the FDA.

In 2005, we reported the first-generation process for the preparation of **1** on a large scale⁴ (Scheme 1). In this approach, the stereochemistry of **1** is derived from β -hydroxy acid **3**, which is prepared using asymmetric hydrogenation of the requisite β -keto ester **2**. The hydroxyl group of **3** is then transformed into protected amino acid **5** through several steps. **1** is obtained after coupling **5** with triazolopiperazine **6** followed by deprotection of the amino group.

The first-generation route provided a means to prepare large quantities (>100 kg) of sitagliptin to support the early safety and clinical studies of this compound. Despite the overall yield being quite high at 52%, multiple steps and isolations led to the production of large amounts of waste. In particular, the EDC coupling-Mitsunobu sequence employed to transform the hydroxyl group of **3** to the masked amino group of **4** provided poor atom economy and was a major contributor to the overall waste output of the synthesis. These reasons inspired us to search for a more efficient and environmentally friendly route for the preparation of **1**.

The central problem of the first-generation route essentially lies in the tortuous nature of creating the β -amino acid moiety via asymmetric hydrogenation of a β -keto ester intermediate. We envisioned that a more direct synthesis could arise from enantioselective hydrogenation of an N-unfunctionized/unprotected enamine to afford the desired β -amino amide or ester directly (Scheme 2).⁵ However, at the time of this work the literature precedence for this type of transformation was limited to enamines that were protected with an N-acyl group such as **8**.^{6,7} The presence of an N-acyl group was viewed as necessary to allow the hydrogenation of an enamine substrate to occur with high enantioselectivity and reactivity. Unfortunately, the use of N-acyl enamines for the preparation of **1** is not attractive and represents a major drawback; not only are these substrates

[†] Merck Research Laboratory.

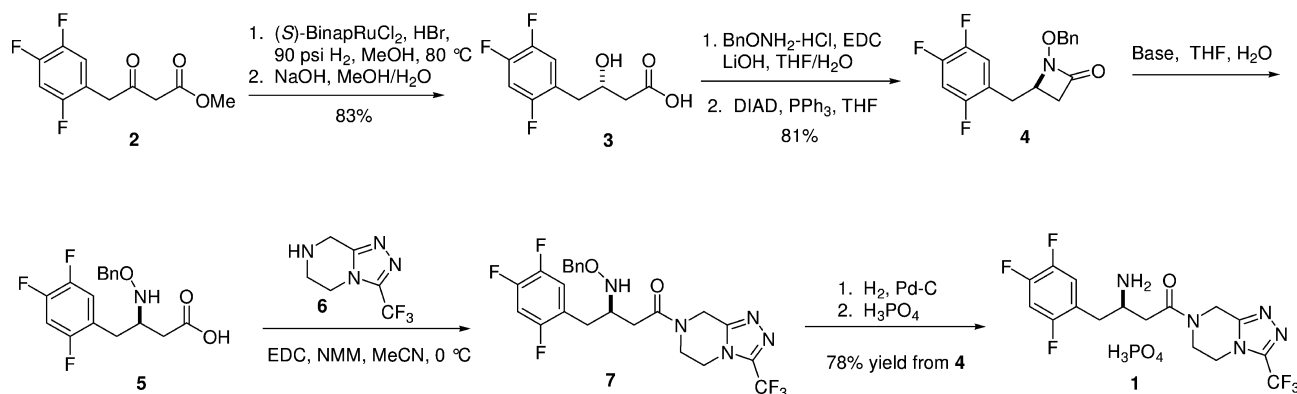
[‡] Solvias AG.

- (1) (a) International Diabetes Federation (IDF), *Diabetes Atlas*, 3rd Edition, Dec, 2006; <http://www.iodf.org/diabetes.asp>. (b) Andrews, M. *U.S. News World Rep.* **2009**, *9*.
- (2) For leading references, see: (a) Thornberry, N. A.; Weber, A. E. *Curr. Topics Med. Chem.* **2007**, *7*, 557–568. (b) Gwaltney, S. L. II.; Stafford, J. A. *Annu. Rep. Med. Chem.* **2005**, *40*, 149–165. (c) Ahrén, B.; Landin-Olsson, M.; Jansson, P. A.; Svenson, M.; Holmes, D.; Schweizer, A. *J. Clin. Endocrinol. Metab.* **2004**, *89*, 2078–2084. (d) Weber, A. *J. Med. Chem.* **2004**, *48*, 4135–4141.
- (3) (a) Kim, D.; et al. *J. Med. Chem.* **2005**, *48*, 141–151. (b) Herman, G. A.; Stein, P. P.; Thornberry, N. A.; Wagner, J. A. *Clin. Pharmacol. Therap.* **2007**, *81*, 761–767.
- (4) Hansen, K. B.; Balsells, J.; Dreher, S.; Hsiao, Y.; Kubryk, M.; Palucki, M.; Rivera, N. R.; Steinhuebel, D.; Armstrong, J. D., III.; Askin, D.; Grabowski, E. J. *J. Org. Process Res. Dev.* **2005**, *9*, 634–639.

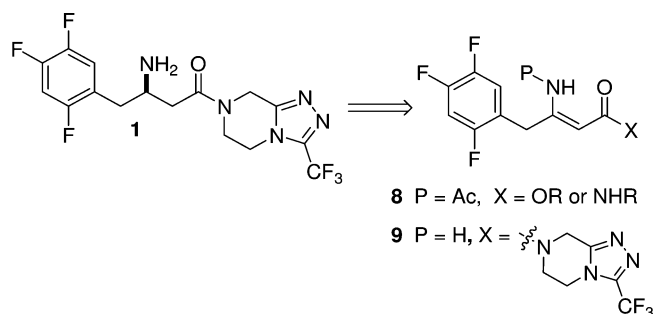
- (5) For preliminary communication, see: (a) Hsiao, Y.; Rivera, N. R.; Rosner, T.; Krska, S. W.; Njolito, E.; Wang, F.; Sun, Y.; Armstrong, J. D., III.; Grabowski, E. J. J.; Tillyer, R. D.; Spindler, F.; Malan, C. *J. Am. Chem. Soc.* **2004**, *126*, 9918–9919.

- (6) For previous examples of asymmetric hydrogenation of electron-rich N-alkyl and N,N-dialkyl enamines, see: (a) Lee, N. E.; Buchwald, S. L. *J. Am. Chem. Soc.* **1994**, *116*, 5985–5986. (b) Tararov, R.; Kadyrov, V. I.; Riermeier, T. H.; Holz, J.; Börner, A. *Tetrahedron Lett.* **2000**, *41*, 2351–2355. (c) Seido, N.; Nishikawa, T.; Sotoguchi, T.; Yuasa, Y.; Miura, T. Kumobayashi, H., U.S. Patent 5,859,249, 1999.

Scheme 1. First-Generation Process of Sitagliptin (1)



Scheme 2. Retro-Synthetic Analysis



with high *E/Z* ratio hard to prepare, but an extra step is also required to deprotect the resulting hydrogenated *N*-acylated amine products under relatively harsh conditions to reveal the free amino functionality. At this point, it became clear that the ideal enamine precursor for the next generation synthesis would be an intermediate such as **9**, which incorporates the entire backbone of sitagliptin including the heterocyclic triazole moiety. In addition, placing the asymmetric transformation as the final step of the synthesis was also envisioned to maximize the utilization of a valuable chiral catalyst.

Thus, our strategy essentially reduced the problem of developing a new route to prepare sitagliptin into three efforts. First, it was necessary for us to develop a short, concise synthesis of dehydrositagliptin (**9**) in order to show advantages over the first-generation synthesis. Second, we needed to discover a metal catalyst that could effect a synthetic target driven, unprecedented reduction of unprotected enamine amides with high enantioselectivity and yield at low enough catalyst loadings to render

the synthesis cost-effective. Last, to meet the high purity specifications required for acceptable use as a chronically administered drug, a robust process to isolate **1** had to be developed. This article describes the successful realization of all of these goals, resulting in an extremely efficient synthesis of **1**.⁸

Results and Discussion

One-Pot Preparation of 9. The approach taken to prepare **9** utilized the ability of Meldrum's acid (**10**) to act as an acyl anion equivalent.⁹ By capitalizing on the ability of **10** to acylate, decarboxylate, and form amides under mild conditions, a one-pot process to prepare the requisite β -keto amide **14** from 2,3,5-trifluorophenyl acetic acid (**11**), triazolopiperazine **6**, and **10** was first developed (Scheme 3). This process involves the activation of **11** by formation of a mixed anhydride with pivaloyl chloride, in the presence of **10**, *i*-Pr₂NEt, and a catalytic amount of dimethylamino pyridine (DMAP) in acetonitrile to form Meldrum's acid adduct **12**. Treatment of **12** with **6** results in formation of β -keto amide **14**. In order to obtain a streamlined preparation of **9**, the overall sequence was studied in detail.

Kinetic studies¹⁰ showed that formation of the amide **9** occurred via degradation of free acid **12** to an oxo-ketene intermediate **13**. By ascertaining the effect of pH through kinetic and spectroscopic studies, a high level of control over this sequence was achieved.¹⁰ In practice, excess *i*-Pr₂NEt was charged in the first step to completely convert the product **12** to its Hunig's base salt. Maintaining **12** as its stable anionic form to minimize its decomposition was one of the keys to make this process robust.¹¹ Following the full consumption of acid **11**, the reaction pH was then lowered with the addition of a substoichiometric amount of CF₃CO₂H (typically 0.3 equiv), which facilitated the liberation of free acid **12** and therefore the formation of ketene **13**. The use of triazole HCl salt **6** to capture **13** allowed recycling/providing 1 equiv of H⁺, which converted the Hunig's salt of **12** to its free acid as 1 equiv each of amide **14** and protonated Hunig's base was formed/liberated, respectively. Thus, the H⁺ cycled in the process became the key for optimal reaction performance.

(7) For reviews about the status of the syntheses of β -amino acids prior to the work described here, see: (a) Abdel-Magid, A. F.; Cohen, J. H.; Maryanoff, C. A. *Curr. Med. Chem.* **1999**, *6*, 955–970. (b) Drexler, H.-J.; You, J.; Zhang, S.; Fischer, C.; Baumann, W.; Spannenberg, A.; Heller, D. *Org. Process Res. Dev.* **2003**, *7*, 355–361. (c) Ma, J.-A. *Angew. Chem., Int. Ed.* **2003**, *42*, 4290–4299.

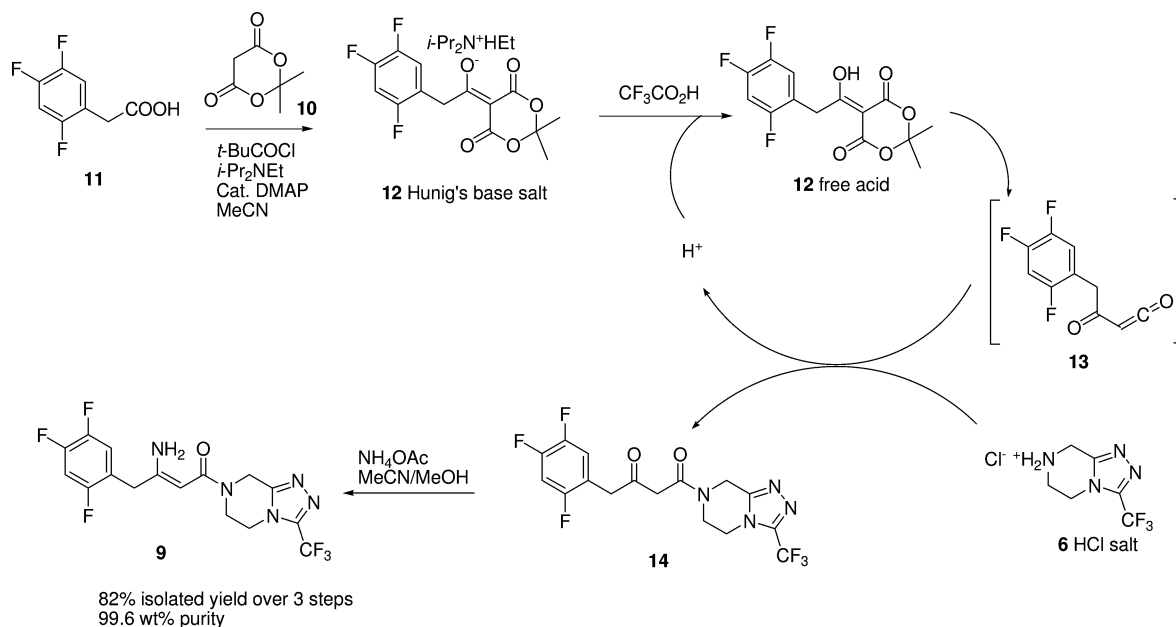
(8) This manufacturing process received the Presidential Green Chemistry Challenge Award (2006) for alternative synthetic pathways and the IChemE Astra-Zeneca Award for excellence in green chemistry and chemical engineering (2005).

(9) For examples, see: (a) Sorensen, U. S.; Falch, E.; Krosgaard-Larsen, P. *J. Org. Chem.* **2000**, *65*, 1003–1007. (b) Hamada, Y.; Kondo, Y.; Shioiri, T. *J. Am. Chem. Soc.* **1989**, *111*, 669–673. (c) Alker, D.; Campbell, S. F.; Cross, P. E.; Burges, R. A.; Carter, A. J.; Gardiner, D. G. *J. Med. Chem.* **1989**, *32*, 2381–2388. (d) Maibaum, J.; Rich, D. H. *J. Med. Chem.* **1989**, *32*, 1571–1576. (e) Shinkai, I.; Liu, T.; Reamer, R. A.; Sletzing, M. *Tetrahedron Lett.* **1982**, *23*, 4899–4902. (f) Mohri, K.; Oikawa, Y.; Hirao, K.-I.; Yonemitsu, O. *Chem. Pharm. Bull.* **1982**, *30*, 3097–3105. (g) Houghton, R. P.; Lapham, D. J. *Synthesis* **1982**, 451–452.

(10) For detailed mechanistic studies, see: (a) Xu, F.; Armstrong, J. D., III.; Zhou, G. X.; Simmons, B.; Hughes, D.; Ge, Z.; Grabowski, E. J. J. *J. Am. Chem. Soc.* **2004**, *126*, 13002–13009.

(11) Meldrum adduct **12**, with a pKa of 3.1 as measured by titration in water at ambient temperature, is not stable in solution as its free acid. However, the anion of **12**, which could be formed with Hunig's base, is quite stable.

Scheme 3. One-Pot Synthesis of Dehydrositagliptin (9)



This one-pot process could be run in highly concentrated MeCN (ca. 1.75 M) to afford β -keto amide **14** in 90% assay yield over the two steps. Although the keto amide **14** could be isolated at this point as a crystalline solid (see Supporting Information), a through process to prepare the enamine amide **9** directly was more desirable. However, attempts to form **9** in the crude acetonitrile reaction solution by charging ammonium salts were not promising due to slow conversion, presumably because of the low solubility of ammonium salts in MeCN. After several experiments, we were glad to find that the formation of **9** could be achieved cleanly by introducing MeOH into the system to increase the conversion, as well as the reaction rate. Thus, without any workup, NH_4OAc along with MeOH was mixed with the crude reaction mixture **14**. Upon heating to 45 °C, the desired product **9** crystallized from the reaction mixture as the reaction proceeded. Upon cooling to 0–5 °C, **9** was directly isolated as a white crystalline solid through a simple filtration, thereby eliminating the need for aqueous workup and minimizing waste generation. It is worthwhile to note that only the *Z* isomer was formed during the reaction.

Thus, **9**, which contains the entire structure of sitagliptin **1** save for two hydrogen atoms, can be prepared in an easily operated one-pot process. This chemistry affords **9** in 82% overall isolated yield with 99.6 wt % purity through a simple filtration. The quality of the material prepared in this fashion was found to be excellent in terms of its performance¹² in the subsequent hydrogenation, and no further purification was required on scale.

Enantioselective Hydrogenation of 9. At the inception of this work, only the asymmetric hydrogenation of *N*-acyl enamines was documented in the literature.⁶ We first designed a small focused screen to assess the feasibility of asymmetric hydrogenation of free enamine **9**. The screen started with a relatively

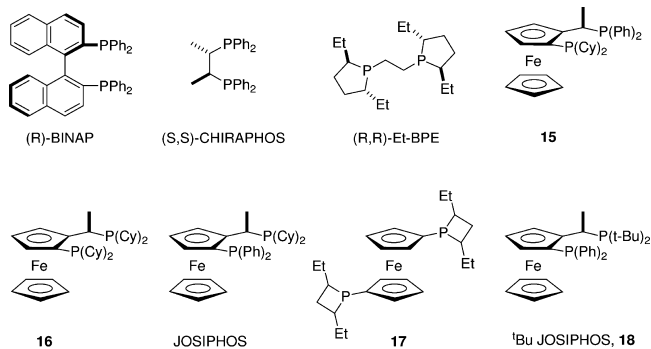
Table 1. Initial Screening Results of Enantioselective Hydrogenation of **9**

Entry	Metal precursor	Ligand	Conv (%)	ee (%) ^a
1	$[\text{Ir}(\text{COD})\text{Cl}]_2$	(R)-BINAP	65	4
2	$[\text{Ir}(\text{COD})\text{Cl}]_2$	(S,S)-CHIRAPHOS	28	4
3	$[\text{Ir}(\text{COD})\text{Cl}]_2$	(S,S)-JOSIPHOS	35	8
4	$[\text{Ir}(\text{COD})\text{Cl}]_2$	(R,R)-Et BPE	33	4
5	$[\text{Ru}(\text{COD})\text{Cl}]_2$	(R)-BINAP	18	-
6	$[\text{Ru}(\text{COD})\text{Cl}]_2$	(S,S)-CHIRAPHOS	1	-
7	$[\text{Ru}(\text{COD})\text{Cl}]_2$	(S,S)-JOSIPHOS	6	-
8	$[\text{Ru}(\text{COD})\text{Cl}]_2$	(R,R)-Et BPE	1	-
9	$[\text{Rh}(\text{COD})_2\text{OTf}]$	(R)-BINAP	0	-
10	$[\text{Rh}(\text{COD})_2\text{OTf}]$	(S,S)-CHIRAPHOS	0	-
11	$[\text{Rh}(\text{COD})_2\text{OTf}]$	(S,S)-JOSIPHOS	>99	86
12	$[\text{Rh}(\text{COD})_2\text{OTf}]$	(R,R)-Et BPE	40	38
13	$[\text{Rh}(\text{COD})_2\text{OTf}]$	15	90	6
14	$[\text{Rh}(\text{COD})_2\text{OTf}]$	16	>99	72
15	$[\text{Rh}(\text{COD})_2\text{OTf}]$	17	>99	89
16	$[\text{Rh}(\text{COD})_2\text{OTf}]$	<i>t</i> -Bu JOSIPHOS 18	>99	95

^a Measured by HPLC analysis: Diacel AD-H column, 5 μm particle size, 250 \times 4.6 mm, 35 °C; isocratic mobile phase: EtOH/hexane/ $\text{Et}_2\text{NH}/\text{H}_2\text{O}$ = 600:400:1:1; flow rate: 0.8 mL/min; UV detection: 268 nm.

small set of commercially available chiral biphosphines (Table 1). The metal precursors investigated focused on Ir, Ru, and Rh salts, mainly because of their demonstrated performance in asymmetric hydrogenation. Screening was carried out in MeOH under a moderately low pressure of hydrogen (50 psig) at 50 °C. Catalyst loading was kept high (5 mol %) in order to facilitate observation of conversion.

(12) Interestingly, the trace amount of NH_4Cl in the isolated **9** turned out to be beneficial for the subsequent hydrogenation in terms of reaction rate and yield. For more detailed discussion about the function of NH_4Cl in sitagliptin hydrogenation, see: (a) Clausen, A. M.; Dziadul, B.; Cappuccio, K. L.; Kaba, M.; Starbuck, C.; Hsiao, Y.; Dowling, T. M. *Org. Process Res. Dev.* **2006**, *10*, 723–726.



Astonishingly, the screening results not only showed a trend of enantioselectivities but also gave us a very direct hit. The results are summarized in Table 1. While Ir and Ru catalysts gave poor results, [Rh(COD)₂OTf], in particular with ferrocenyl-based JOSIPHOS-type catalysts, afforded both high conversion and enantioselectivity. In particular, the *tert*-butyl variant, ligand **18**, was found to provide **1** in 99% conversion with 95% ee. In addition, using the more readily available [Rh(COD)Cl]₂ dimer as a precursor instead of [Rh(COD)₂OTf] afforded identical results.

Further exhaustive screening¹³ revealed that other ligands, even ones outside the ferrocenyl structural class, could effect this transformation with high enantioselectivity. The selected ligands that provided the highest levels of enantioselectivity in conjunction with [Rh(COD)Cl]₂ are shown in Figure 1.

Given an overall consideration of the yield, enantioselectivity, and reaction rate, as well as cost of the ligand, we decided to choose the [Rh(COD)Cl]₂-^tBu-JOSIPHOS (**18**) combination for further development. At this point, although we had achieved proof of concept on the strategy to prepare **1** directly from **9**, a large amount of optimization remained in order for the process to be viable for the commercial manufacture of **1**.

Our preliminary kinetic studies showed that the reaction rate slowed down over the course of the hydrogenation. To understand this decreasing rate issue better, in situ FT-IR technology was applied to explore whether binding of the hydrogenated product **1** to the rhodium metal catalyst could have an adverse effect on the reaction rate and the asymmetric environment of the catalyst under completely homogeneous reaction conditions. Although the observed enantioselectivity did not change throughout the course of the hydrogenation, weak product inhibition of the catalyst was confirmed by a product-doping experiment unambiguously (Figure 2). We observed lower reaction rates with increasing amounts of product present at the beginning of the reaction. The experimental data were

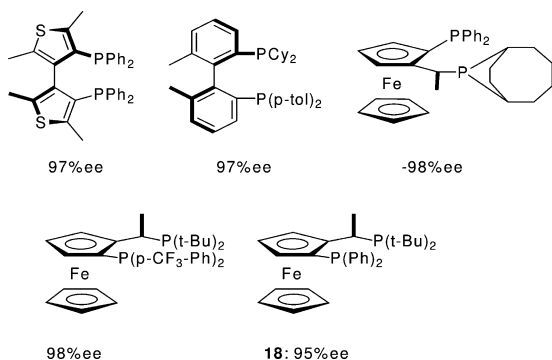


Figure 1. Selected results of asymmetric hydrogenation of **9** with chiral ligands/[Rh(COD)Cl]₂.

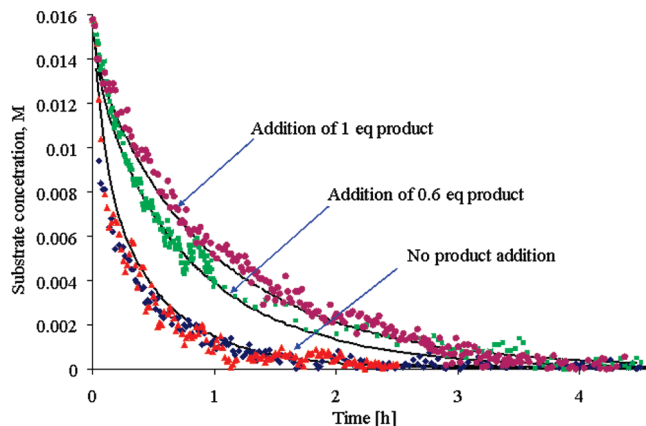


Figure 2. Kinetic effects with product inhibition on hydrogenation. Plots of concentration of **9** in MeOH vs time based on FT-IR data (dotted lines) and modeled profiles (solid lines).¹⁴ All reactions were homogeneous with the initial concentration of **9** at 0.016 M under 100 psig of hydrogen.

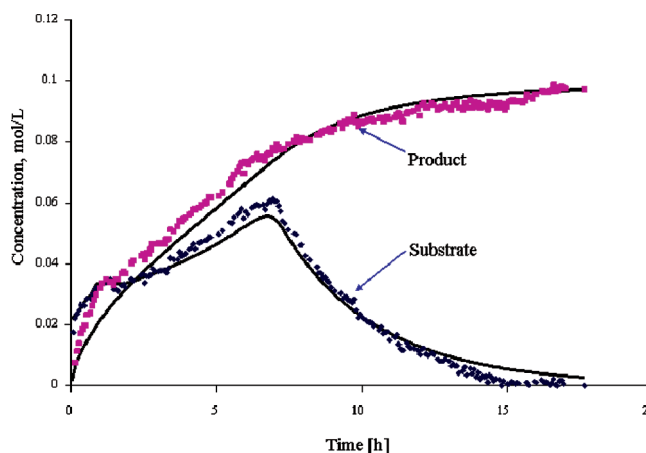


Figure 3. Hydrogenation reaction profile. Plots of concentration of **1** and **9** in MeOH vs time based on FT-IR data (dotted lines) and modeled profiles (solid lines).¹⁴ The reaction was run at 0.3 M under 100 psig of hydrogen.

modeled¹⁴ to reaction kinetics with product inhibition with good correlation as indicated by the solid black lines. Fortunately, the product inhibition was not strong enough to make the reaction impractical.

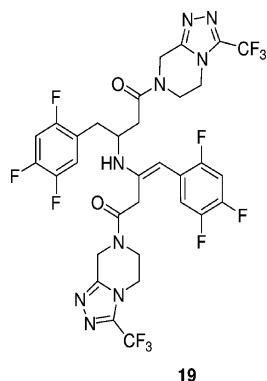
In order to maintain efficient volumetric productivity of the process, the hydrogenation was thus carried out as a slurry in MeOH. A typical reaction profile as monitored by in-line FTIR is shown in Figure 3 (dotted lines). The concentration of enamine **9** in solution increased slowly as the reaction proceeded, presumably due to increased solubility of **9** in methanol as a result of the presence of the amine product. After about 7 h, the reaction mixture became homogeneous. Approximately 80% of the substrate was consumed at this point. It took another 8–10 h to reach >98% conversion. The profiles of enamine **9**

(13) In collaboration with Solvias AG, Switzerland, extensive screenings were carried out to search for the most suitable catalyst for this hydrogenation.

(14) Experimental profiles were fitted to a Michaelis–Menten-type kinetic model with product inhibition ($r = k'K_A[9]/(1 + K_A[9] + K_P[1])$) using DynoChem. Fitting provided a wide range of solutions. However, K_P/K_A ranges typically from 30 to 35. A good fit was achieved for reaction profiles shown in Figures 2 and 3 as $k' = 2.09 \times 10^3 \text{ h}^{-1}$, $K_A = 150 \text{ L/mol}$, and $K_P = 5.15 \times 10^3 \text{ L/mol}$.

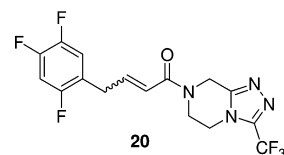
and the free base **1** product were successfully predicted when kinetic constants from diluted conditions were applied, and a linear proportional solubility profile to the amount of product in solution was superimposed (Figure 3 solid line).¹⁴ The effective extrapolation of results from diluted conditions to slurry process conditions provided additional confidence in understanding the reaction and its constraints for the subsequent large scale productions.

During the optimization, we discovered that a small amount (0.15–0.3 mol %) of NH_4Cl was necessary to achieve consistent performance in terms of both ee and conversion rate.¹² However, the addition of excess NH_4Cl had a deleterious effect, significantly increasing the formation of the dimer byproduct **19**. While NH_4Cl was present in the substrate as a process impurity, introducing an additional small amount of NH_4Cl ¹⁵ ensured robustness of hydrogenation on scale. The effect has been studied in depth in terms of producing consistent hydrogenation results, but the mechanism is not clear. In addition, we also discovered that many other acidic additives, such as tartaric acid and phosphoric acid, can increase the hydrogenation rate significantly without affecting enantioselectivity.¹⁶ However, all of these acidic additives resulted in the formation of significant amount of dimer **19**.



The chemistry was further optimized to lower catalyst loading, increase volumetric productivity, and achieve an adequate reaction rate. Determining the optimum reaction volume was driven by the relatively low solubility of enamine **9** in MeOH. If the reaction was carried out in a thick slurry of **9**, inconsistent results were obtained presumably due to mass-transfer issues. The best balance was achieved when the reaction was performed in 8 L of MeOH per kg of **9**. At this concentration and under 100 psig of hydrogen, the catalyst loading was reduced to 0.3 mol % with no impact on selectivity or yield. The rate under these conditions was sufficient to achieve complete conversion of **9** in 16 h. Attempts to improve the performance of the catalyst by increasing the temperature further to 70 °C led to a significant reduction in enantioselectivity (down to 90% ee), and a significant amount of **20** formed by elimination of ammonia from **1**.

Although the use of 0.3 mol % catalyst already made the asymmetric hydrogenation approach viable from an efficiency and cost perspective, the chiral catalyst still represented an



important cost factor in our synthesis. In order to improve the efficiency of the process further, we started to explore the function of hydrogen pressure. A plot of reaction conversion vs a series of catalyst loadings for three different reaction pressures is shown in Figure 4. We were pleased to find that increasing the pressure to 250 psig allowed for a further reduction of the catalyst loading to 0.15 mol % without sacrificing yield, ee, or reaction rate at 50 °C. The reduction in catalyst loading, and therefore the cost of the synthesis, by simply increasing hydrogen pressure demonstrated the power of asymmetric hydrogenation to set the stereochemistry of **1**.

In order to gain some insight into the mechanism of this transformation, we performed the asymmetric transformation using deuterium instead of hydrogen. The obtained product **22** had incorporated deuterium only in the β -position (Scheme 4). An NMR study also revealed that there was no H–D exchange between methanol- d_4 and **1** at either the α or β positions. These results suggested that the hydrogenation plausibly proceeded through the imine tautomer (Scheme 4).

Worthy of note is the operational ease of this hydrogenation on large scale, although it involves an oxygen-sensitive transition metal complex. Both the metal precursor $[\text{Rh}(\text{COD})\text{Cl}]_2$ and the ligand **18** are air-stable solids and can be stored for prolonged periods. The active catalyst could be generated in situ by mixing the two solids in degassed reaction solvent or simply adding the two solids to the reaction slurry of **9** in MeOH under nitrogen atmosphere.

In summary, hydrogenation of **9** in the presences of NH_4Cl (0.15 mol %), $[\text{Rh}(\text{COD})\text{Cl}]_2$ (0.15 mol %), and ^tBu JOSIPHOS **18** (0.155 mol %) in MeOH under 250 psig of hydrogen at 50 °C for 16–18 h was proved to be extremely robust and afforded **1** in 98% yield and 95% ee reproducibly. The crude MeOH reaction solution was then taken through the purification step.

End Game. In order to complete the synthesis, the dissolved rhodium and undesired enantiomer, as well as other process impurities, needed to be removed during the isolation of **1** to meet the pharmaceutical industry standards. Thus, the use of solid absorbents to selectively recover/remove the expensive soluble rhodium from the crude reaction stream became attractive.

After screening various solid absorbents, we found that Ecosorb C-941¹⁷ was the optimal choice. Ecosorb C-941, a polymer impregnated with activated carbon, is inexpensive and possesses excellent filtration properties. Most importantly, treatment of the crude hydrogenation stream of **1** with as little as 10 wt % of Ecosorb resulted in near complete removal of the dissolved rhodium.¹⁸ Interestingly, the efficiency of this rhodium recovery was observed to decrease if the reaction solution was exposed to air for prolonged periods, most likely due to oxidation of the catalyst complex; however, maintaining an inert atmosphere was straightforward on plant scale. Most importantly, nearly all of the rhodium utilized in the process

(15) Optimal performance was achieved with a mole ratio of 1:1 NH_4Cl /catalyst.

(16) For these experiments, no additional NH_4Cl was added and the enamine **9** was purified through recrystallization. The observed acid additive effects on the reaction rate were clearly confirmed with controlled experiments by using the same lot of enamine **9** in the absence of acid additives.

(17) Commercial source of Ecosorb C-941: Graver Technologies, Glasgow, DE 19702.

(18) The Fe and Rh residue in the isolated sitagliptin free base is typically <20 ppm.

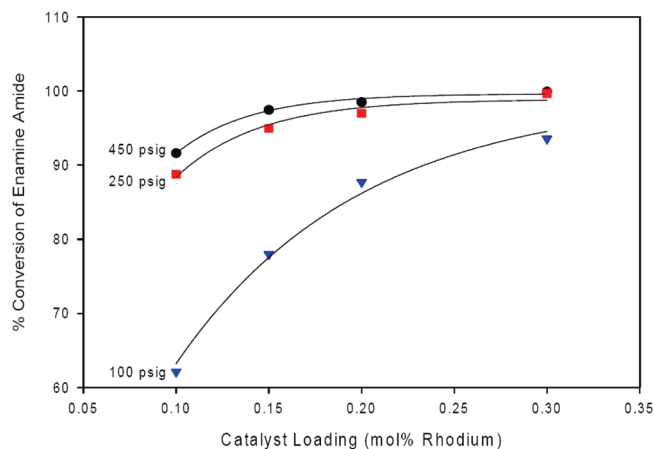
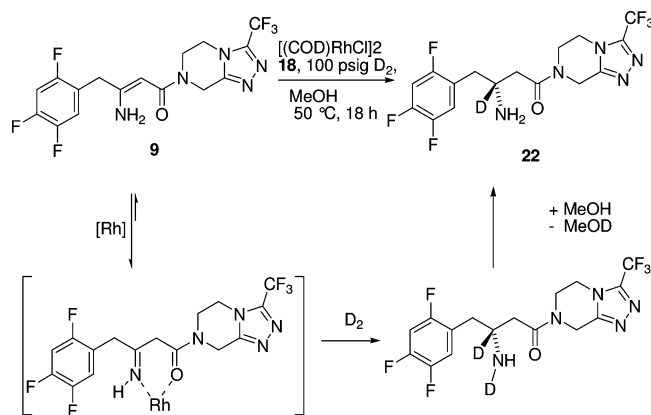


Figure 4. Effects of reaction pressure and catalyst loading on conversion. Plots of conversion of **9** vs amounts of catalyst Rh(I)-**18** at 50 °C after 14 h at different pressures of hydrogen.

Scheme 4. Plausible Mechanism for the Asymmetric Hydrogenation of **9**



could be recovered from the treated solids, which further made the process more cost-effective on manufacturing scale.

Several options were explored for removal of the undesired enantiomer through crystallization. The minor enantiomer of **1** was not rejected when **1** was isolated as its phosphate salt, due to the formation of a stable racemate crystal form. After several experiments, we found that isolation of **1** as its free base was a viable approach for upgrading the enantiomeric purity. Solid-state characterization of both enantiomerically pure **1** and its racemic mixture revealed that racemate **1** crystallized as a conglomerate and was much more soluble than enantiomerically pure **1**.

Since the free base **1** is prone to decomposition under thermal conditions (*vide ante*), to ensure stability of **1** the crude Ecosorb-treated methanol stream was solvent switched to *i*-PrOH via vacuum distillation below 45 °C. After nearly all of the methanol was removed, heptane was then added. Thus, crystalline free base **1** was isolated in 84% yield with an upgrade in enantiomeric excess from 95% ee to >99% ee. Finally, **1** was isolated as its phosphate monohydrate from aqueous *i*-PrOH in 96% yield with >99.9 A% purity and nearly perfect ee.

Conclusion

In summary, a highly efficient, asymmetric synthesis of **1**, which has been implemented on manufacturing scale, has been described. The entire synthesis is carried out with a minimum

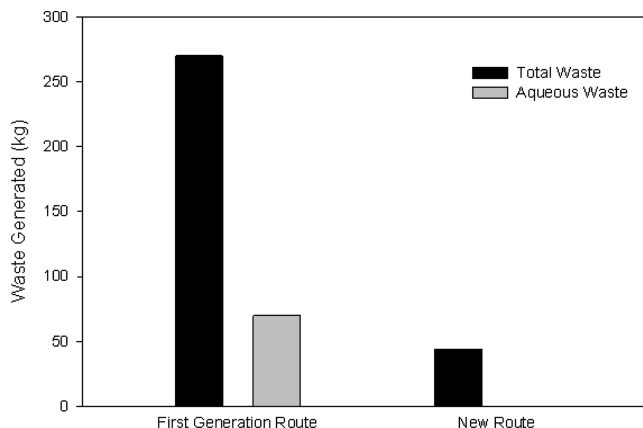


Figure 5. Waste generation per kilogram of sitagliptin produced. For this analysis, the volumes of pilot plant waste streams were compared between the two routes, once normalized to a per kilogram of **1** produced. The total waste was analyzed, as well as the amount of aqueous waste streams.

number of operations: a one-pot process affords the crystalline dehydrositagliptin **9** in >99.6 wt %; the highly enantioselective hydrogenation of **9** in the presence of as low as 0.15 mol % ^tBu JOSIPHOS-Rh(I) gives **1** in high yield and >95% ee. After all of the precious metal catalyst is selectively recovered/removed from the process stream, **1** is isolated as its free base, which was then converted to its final desired pharmaceutical form, its monohydrate phosphate salt, in >99.9 A% purity and >99.9% ee. The use of low Rh(I) loading for asymmetric hydrogenation in combination with an ease of recovery of the precious rhodium metal made this process highly cost-effective. The overall yield of this process is up to 65%.

The route described in this manuscript is a good example of a synthetic target driving the discovery of new chemistries, enantioselective hydrogenation of unprotected enamine amide. The route contains all of the elements required for a manufacturing process. The route essentially is short and efficient and prepares **1** with the high quality required for pharmaceutical use. More importantly, by devising a more straightforward approach to prepare **1**, the amount of waste produced in the process was reduced significantly. Figure 5 compares the waste produced for the production of **1** for both the first generation route and the asymmetric hydrogenation route. In comparison to the first-generation route, the total waste generated per kilogram of **1** produced in this environment-friendly 'green' process is reduced from 250 kg to 50 kg. Most strikingly, the amount of aqueous waste produced in the process was reduced to zero. The drastic reductions in waste, realized over virtually the entire product lifetime for **1**, coupled with the new chemistry discovered in this efficient process, led to the awarding of both a Presidential Green Chemistry Award and the ICHME Astra-Zeneca award for sustainability.⁸

Experimental Section

(Z)-3-Amino-1-(3-trifluoromethyl-5,6-dihydro-8H-[1,2,4]triazolo[4,3-a]pyrazin-7-yl)-4-(2,4,5-trifluoro-phenyl)-but-2-en-1-one (**9**). 2,4,5-Trifluorophenylacetic acid (**11**, 2.5 kg, 13.15 mol), Meldrum's acid (**10**, 2.09 kg, 14.46 mol), DMAP (128.5 g, 1.052 mol), and acetonitrile (7.5 L) were charged into a 50 L three-neck flask. *N,N*-Diisopropylethylamine (4.92 L, 28.27 mol) was added in portions at room temperature while maintaining the temperature below 50 °C. Pivaloyl chloride (1.78 L, 14.46 mol) was added dropwise over 1–2 h while maintaining the temperature below 55 °C. The reaction was aged at 45–50 °C for 2–3 h. Triazole hydrochloride **6** (3.01

kg, 13.2 mol) was added in one portion at 40–50 °C. Trifluoroacetic acid (303 mL, 3.95 mol) was added dropwise, and the reaction solution was aged at 50–55 °C for 6 h. 90% solution assay yield of **14** (4.81 kg).

A solution of NH₄OAc (0.91 kg, 11.81 mol) in MeOH (27 L) was heated to 45 °C. About 10% of the above ketoamide **14** crude solution was then added dropwise over 30 min. The reaction mixture was stirred at 45 °C for 1.5 h, and the batch was then seeded with **9** (140 g). After 30 min at 45 °C, the remaining of the crude **14** solution was added dropwise over 3–6 h. After additional 3 h age, MeOH (12 L) was charged over 2 h while maintaining the batch temperature at 40–45 °C. The slurry was then cooled to 0–5 °C over 3–4 h and aged for an additional 1 h before filtration. The wet cake was washed with 29 L of cold methanol (0 °C) and dried at ambient temperature in a vacuum oven to afford 4.37 kg of white crystalline **9** (99.6 wt %), 82% yield. ¹H-NMR (400 MHz, DMSO-*d*₆): δ 8.48 (s, br, 1H), 7.50 (m, 2H), 6.82 (s, br, 1H), 4.90 (s, 1H), 4.85 (s, 2H), 4.14 (t, *J* = 5.1 Hz, 2H), 3.90 (t, *J* = 5.1 Hz, 2H), 3.44 (s, 2H). ¹³C-NMR (100 MHz, CDCl₃): δ 168.9, 160.1, 155.6 (ddd, *J* = 243.7, 10.0, 1.7 Hz), 151.4, 148.1 (dt, *J* = 247.4, 13.9 Hz), 145.9 (ddd, *J* = 241.5, 12.1, 3.3 Hz), 142.4 (q, *J* = 38.9 Hz), 121.9 (ddd, *J* = 18.6, 6.3, 4.2 Hz), 118.6 (dd, *J* = 19.7, 5.5 Hz), 118.5 (q, 270.6 Hz), 105.6 (dd, *J* = 28.9, 21.4 Hz), 81.0, 43.5, 34.1. Anal. Calcd for C₁₆H₁₃F₆N₅O: C, 47.41; H, 3.23; N, 17.28; Found: C, 47.42; H, 3.16; N, 17.20.

5-[1-Hydroxy-2-(2,4,5-trifluorophenyl)ethylidene]-2,2-dimethyl-1,3-dioxane-4,6-dione (12). mp 117 °C (dec). ¹H-NMR (400 MHz, CDCl₃): δ 15.50 (s, 1H), 7.14 (m, 1H), 6.96 (m, 1H), 4.45 (s, 2H), 1.76 (s, 6H). ¹³C-NMR (100 MHz, CDCl₃): δ 192.76, 170.66, 160.42, 156.47 (ddd, *J*_{CF} = 245.7, 9.6, 2.4 Hz), 149.79 (ddd, *J*_{CF} = 251.4, 14.5, 12.0 Hz), 146.90 (ddd, *J*_{CF} = 244.9, 12.0, 3.2 Hz), 119.40 (dd, *J*_{CF} = 19.3, 5.6 Hz), 117.41 (ddd, *J*_{CF} = 18.5, 5.6, 4.0 Hz), 105.80 (dd, *J*_{CF} = 28.1, 20.9 Hz), 105.63, 91.99, 34.59, 27.06. HRMS: Calcd for C₁₄H₁₁F₃O₅–H *m/z* 315.0480; Found 315.0478.

4-Oxo-4-[3-(trifluoromethyl)-5,6-dihydro[1,2,4]triazolo[4,3-*a*]pyrazin-7(8*H*)-yl]-1-(2,4,5-trifluorophenyl)butan-2-one (14). In CD₃CN solution, **14** exists as a 4:3 mixture of amide rotamers (hindered rotation around the nitrogen–carbonyl bond). Severe overlap of signals does not permit unequivocal assignment of each rotamer. Assignments are grouped (when necessary) and rotamers (major/minor/both) denoted. Complexity due to ¹⁹F spin–spin coupling does not permit assignment of all ¹³C resonances, therefore, select ¹³C data are presented. The structure shown is the major rotamer in solution. ¹H NMR (400 MHz, CD₃CN): δ 7.23–7.07 (overlapping m, 2H, both), 4.91 (s, 2H, major), 4.81 (s, 2H, minor), 4.16 (t, *J* = 5.6 Hz, 2H, major), 4.11 (t, *J* = 5.6 Hz, 2H, minor), 4.00 (t, *J* = 5.6 Hz, 2H, minor), 3.92 (s, 2H, major), 3.91 (s, 2H, minor), 3.83 (t, *J* = 5.6 Hz, 2H, major), 3.80 (s, 2H, major), 3.78 (s, 2H, minor). ¹³C NMR (100 MHz, CD₃CN, selected data): δ 201.43 (both), 167.37 (minor), 167.27 (major), 151.88 (major), 151.53 (minor), 48.88 (minor), 48.81 (major), 44.65 (major), 44.19 (minor), 43.86 (minor), 43.08 (major), 43.00 (both), 39.82 (major), 38.81 (minor). HRMS: Calcd for C₁₆H₁₂F₆N₄O₂–H *m/z* 405.0786; Found 405.0786.

7-[(3*R*)-3-Amino-1-oxo-4-(2,4,5-trifluorophenyl)butyl]-5,6,7,8-tetrahydro-[3-(trifluoromethyl)-1,2,4-triazolo[4,3-*a*]pyrazine Phosphate (1:1) Monohydrate (1). To a slurry of **9** (405.3 g, 1.0 mol) and ammonium chloride (80 mg, 1.5 mmol) in methanol (3.25 L) was added **18** (52 mg, 1.55 mmol) followed by [(COD)RhCl]₂ dimer

(23 mg, 1.5 mmol). The slurry was N₂ degassed and aged with agitation for 1 h, then heated to 50 °C and hydrogenated under 250 psig hydrogen pressure. After 15–17 h, the reaction mixture was cooled to ambient temperature. Ecosorb C-941¹⁷ (40.5 g) was charged to the batch. The slurry was aged at ambient temperature for 1 h before filtration. The wet cake was washed with methanol (1.2 L). The filtrate was solvent-switched to isopropanol via distillation under reduced pressure to a final volume of ~1.1 L, while maintaining the batch temperature below 40 °C. After the distillation, the batch was maintained at 40 °C for 1 h, and then cooled to 20–15 °C. Heptane (3.2 L) was added dropwise over 3–4 h. After filtration, the wet cake was washed with 20% isopropanol in heptane (1.2 L) and dried in vacuo at 40 °C to afford free-base **1** in 82% yield (332 g) and >99.9% ee.

To a solution of free-base **1** (407.3 g, 1.0 mol) in isopropanol (1.73 L) and water (0.45 L) was added 45 wt % H₃PO₄ (1.15 mol) dropwise. The resulting slurry was heated to 70–80 °C to dissolve the solids. The batch solution was then cooled to 60–65 °C and seeded with milled phosphate monohydrate **1** (3 g). The batch was agitated for 3 h at 60–65 °C and cooled to ambient temperature over 6 h. Isopropanol (1.26 L) was added dropwise to the batch over 1–2 h. The slurry was then filtered, and the wet cake was washed with aqueous isopropanol (20 wt % water, 1.2 L). The wet cake was dried at ~40 °C in vacuo to give 390 g of phosphate monohydrate **1** in 96% yield (corrected for seed charged). ¹H NMR (600 MHz, D₂O): In D₂O solution, **1** exists as a 4:3 mixture of amide rotamers. Severe overlap of signals does not permit unequivocal assignment of each rotamer. Assignments are grouped (when necessary) and rotamers (major/minor/both) denoted in parentheses. δ 7.06 (overlapping m, 1 H, both), 6.92 (overlapping m, 1 H, both), 4.76 (s, 2 H, minor), 4.75 (d, *J* = 17.6 Hz, 1 H, major), 4.70 (d, *J* = 17.6 Hz, 1 H, major), 4.11 (m, 2 H, major), 4.08 (m, 1 H, minor), 4.03 (m, 1 H, minor), 3.89–3.78 (overlapping m, 2 H, minor; 1 H, both), 3.79 (m, 2 H, major), 2.92 (m, 2 H, both), 2.86–2.79 (overlapping m, 1 H, both; 1 H, minor), 2.79 (dd, *J* = 17.1, 4.9 Hz, 1 H, major), 2.68 (overlapping m, 1 H, both). ¹³C-NMR (150 MHz, D₂O): 170.37 (1C, minor), 170.29 (1C, major), 119.26 (overlapping m, 1C, both), 156.44 (overlapping m, 1C, both), 151.24 (1C, major), 150.70 (1C, minor), 149.39 (overlapping m, 1C, both), 146.64 (overlapping m, 1C, both), 143.97 (q, *J*_{CF} = 40.8 Hz, 1C, minor), 143.86 (q, *J*_{CF} = 40.7 Hz, 1C, major), 118.60 (overlapping m, 1C, both), 117.80 (q, *J*_{CF} = 270.1 Hz, 1C, major), 117.78 (q, *J*_{CF} = 270.2 Hz, 1C, minor), 105.96 (dd, *J*_{CF} = 28.6, 21.2 Hz, 1C, both), 48.38 (1C, both), 43.57 (1C, major), 43.28 (1C, minor), 41.98 (1C, minor), 41.33 (1C, major), 38.89 (1C, major), 38.19 (1C, minor), 33.92 (1C, major), 33.85 (1C, minor), 31.14 (1C, major), 31.04 (1C, minor). HRMS: Calcd for C₁₆H₁₅N₅O₆ [M + H]⁺ 408.1259; Found 408.1264.

Acknowledgment. We thank Mr. A. Houck, Mr. C. Bazaral, and Mr. A. Newell of the Merck High Pressure Laboratory for experimental assistance and Dr. R. Reamer, Dr. P. Dormer, and Ms. L. DiMichele for assistance with NMR studies.

Supporting Information Available: Experimental procedure to isolate **12** and **14**; complete ref 3a. This material is available free of charge via the Internet at <http://pubs.acs.org>.

JA902462Q